7802 *J. Org. Chem.* **1999,** *64,* 7802−7806

Derivatives of *N*-Benzyl-2-phenylpyridinium Bromide, Minimalist Models for Face-to-Face, Center-to-Edge π-Stacking in Water

Christopher B. Martin, Hormuzd R. Mulla, Peter G. Willis, and Arthur Cammers-Goodwin*

University of Kentucky, Department of Chemistry, Lexington, Kentucky 40506-0055

Received May 7, 1999

The substitution pattern of the benzyl ring was varied in preparations of derivatives of *N*-benzyl-2-phenylpyridinium bromide (**1**−**8**). The salts showed monomeric behavior at NMR concentrations in D_2O. The title compounds are discussed in the context of their propensity to intramolecularly stack aromatic substituents in water solvent and in the solid state. The series of derivatives, **1**−**8**, populated similar stacked conformational space in solution. Neither perturbation in the quadrupole moment nor perturbation in donor/acceptor properties of the interacting aromatic rings had observable effects on the solution conformation of **1**−**8**. The propensity of arene and perfluoroarenes to stack in a fact-to-face manner may have been the reason for the minor changes in conformation observed in the solid state. Derivatives **1**−**8** served as a unique tether for arene stacking, consisting of two trigonal and one tetrahedral center.

Introduction

Affinity between aromatic rings is often inferred from physical studies of a wide variety of substances.[1,2] Even though π-stacking is an old argument for conformational stability, progress in understanding its molecular origins has been recent. Experimentally quantifying π-stacking challenges chemists because aromatic moieties interact weakly compared to polar substructures. However, the affinity between derivatives of perfluorobenzene and those of benzene is noteworthy[3] because perfluoro alkanes and the analogous hydrocarbons tend not to misc. Furthermore, fluorocarbons generally boil at lower temperatures than hydrocarbons.[4] The C_6F_6/C_6H_6 heterodimer appears to prefer nearly face-to-face, center-to-center (FFCC) orientation in the solid state. The edge-to-face (EF) or T-shaped C_6H_6 homodimer is the calculated spatial arrangement of minimum energy.[5] Calculations also indicate that the energetic difference between EF and the face-to-face, center-to-edge (FFCE) orientation of the C_6H_6 homodimer is only 0.06 kcal/mol.[6] Gas-phase vibrational spectroscopy hints at a floppy association for the C_6H_6 dimer.[7]

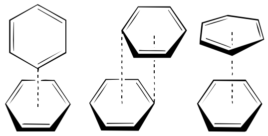

Molecular modeling led to the consideration of the title compounds as minimalist models for the FFCE aromatic interaction in water. The molecules can be considered as tethered aromatic substructures. A water-soluble, sp^3-hybridized three-atom tether,[13] sp^2-hybridized three-atom tethers,[8,14] and the methylene tether[15] have been used to study aromatic interactions. However, this study of two sp^2 centers and one sp^3 center to mediate π-stacking between two aromatic substituents is unique.

Even though the title compounds are simple, exhaustive literature searches did not uncover previous conformational studies. Solid-state studies of 2,6-disubstituted pyridinium derivatives[16] hint that **1**−**8** can adopt both stacked and splayed conformations. The conformations of *N*-benzylpyridinium bromide have been studied in the solid state and with calculations.[17] Apparently, the dihedral angle in these simpler structures analogous to C2−N1−C13−C14 in *N*-benzylpyridinium bromide (see structure **1** for atom numbers) favors 90°.

Other π-stacking models[8] and reports cited above implicate electrostatic moments of aromatic rings as major contributors to π-stacking interactions.[9,10] However, this perspective has been questioned by recent conformational studies on model compounds.[11,12] In agreement with these recent findings, the results of our work do not support arguments for π-stacking that are based solely on the quadrupole moment of the aromatic rings. Derivatives **1**−**8** belonged to a conformationally related

---

(1) Hunter, C. A. *Chem. Soc. Rev.* **1994**, *23*, 101−109.

(2) Breinlinger, E. C.; Rotello, V. M. *J. Am. Chem. Soc.* **1997**, *119*, 1165−66.

(3) Coates, G. W.; Dunn, A. R.; Henling, L. M.; Ziller, J. W.; Lobkovsky, E. B.; Grubbs, R. H. *J. Am. Chem. Soc.* **1998**, *120*, 3641−3649.

(4) Sheppard, W. A.; Sharts, C. M. *Organic Fluorine Chemistry*; W. A. Benjamin Inc.: New York, 1969.

(5) Linse *J. Am. Chem. Soc.* **1992**, *114*, 4366−4373.

(6) Seminario, J. M.; Zacarias, A. G.; Tour, J. M. *J. Am. Chem. Soc.* **1998**, *120*, 3970−3974.

(7) Krätzschmar, O.; Selzle, H. L.; Schlag, E. W. *J. Phys. Chem.* **1994**, *98*, 3501−3505.

(8) Cozzi, F.; Cinquini, M.; Annunziata, R.; Dwyer, T.; Siegel, J. S. *J. Am. Chem. Soc.* **1992**, *114*, 5729−33.

(9) Luhmer, M.; Bartik, K.; Dejaegere, A.; Bovy, P.; Reisse, J. *Bull. Soc. Chim. Fr.* **1994**, *131*, 603−606.

(10) Williams, J. H. *Acc. Chem. Res.* **1993**, *26*, 593−598.

(11) Kim, E.-i., Paliwal, S., Wilcox, C. S., *J. Am. Chem. Soc.* **1998**, *120*, 11192−11193.

(12) Gellman, S. H.; Haque, T. S.; Newcomb, L. F. *Biophys. J.* **1996**, *71*, 3523−26.

(13) Newcomb, L. F.; Haque, T. S.; Gellman, S. H. *J. Am. Chem. Soc.* **1995**, *117*, 6509−6519.

(14) Tanatani, A.; Yamaguchi, K.; Kagechika, H. *J. Am. Chem. Soc.* **1998**, *120*, 6433.

(15) Martinez, A. G.; Barcina, J. O.; Rivas, R. G.; Bach, R. D.; Estevez, C. M.; Glukhovtsev, M. N. *J. Am. Chem. Soc.* **1998**, *120*, 680.

(16) Katritzky, A. R.; Lamba, D.; Spagna, R.; Vaciago, A.; Prewo, R.; Bieri, J. H.; Stezowski, J. J.; Musumarra, G. *J. Chem. Soc., Perkin. Trans. 1* **1987**, 1391−.

(17) Anders, E.; Tropsch, J. G.; Irmer, E.; Sheldrick, G. M. *Chem. Ber.* **1990**, *123*, 321−325.

10.1021/jo9907641 CCC: $18.00

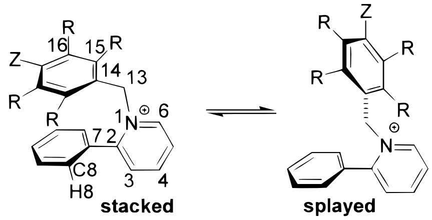

Figure 1. 1 Z, R = H; **2** Z = OMe, R = H; **3** Z = CN, R = H; **4** Z = CF_3, R = H; **5** Z = CF_3, R = F; **6** Z, R = F; **7** Z = NO_2, R = H; **8** Z = Me, R = H. The numbers on **1** denote carbon atoms or bound hydrogen atoms referred to in the text.

set of molecules. Neither perturbation in quadrupole moment nor donor–acceptor character of the benzyl ring had a notable change in solution or solid-state structure. However, solution and solid-state studies indicated a preference for FFCE π-stacked conformations in **1**–**8** over splayed conformations.

The FFCE interaction results from the N1–C2–C7–C8 dihedral angle turning to optimize aromatic interaction between the phenyl and the benzyl substituents. The major contributions to the energy difference between *stacked* and *splayed* (Figure 1) should be $A_{1,3}$-strain[18] and electrostatic or dispersive interactions between the aromatic substituents. Since **1**–**8** will have similar energetic contributions from $A_{1,3}$-strain between the Bn and Ph substituents, we reasoned that studying the conformations of **1**–**8** should reveal population changes in conformation that are purely a function of stacking interactions. Torsional strain should edit both EF and FFCC π-stacking out of the conformational distribution of **1**–**8**. Substituents R and Z were chosen to perturb the electronic character of the benzyl rings in **1**–**8** to determine if electrostatic interactions would affect the distribution of conformers. Evidence for intramolecular stacking in the solid state and in the solution state for **1**–**8** and evidence for the conformational insensitivity to the electronic characteristics of the aromatic rings are presented in this paper.

Results and Discussion

Solubility and Aggregation State. Good water solubility and lack of aggregation made the bromide salts of 2-phenylpyridinium derivatives ideal for NMR studies. Beer's Law was obeyed from concentrations of the NMR studies down to concentrations of the UV detection threshold for **1** (330 nm, $\epsilon = 28.9$ M ± 0.1 M^{-1} cm^{-1}, $R = 0.9997$). The concentration of **1** was varied from 0.113 to 0.003 M for this assay.

Operational Definition of Stacking. EF and FF π-stacking are extremes of a continuum in which the dihedral angle (α in Table 1) between the two planes that contain the arenes is 90 or 0°, respectively. In general, α was below 30° for solid states **1**–**6**. From the hypothetical FF motif, the rings can slide from FFCC stacking to FFCE stacking to nonstacked conformations. The x parameter in Table 1 quantifies this horizontal displacement. The vertical displacement of the ring centroids is the parameter z in Table 1. Good EF stacking has parameters $\alpha > 45°$, $x = 0$ Å, and $z \approx 3.3$ Å. Likewise, good FFCE stacking has $\alpha < 45°$, 1.37 Å $< x < 2.7$ Å, and 3.3 Å $< z < 4.0$ Å. The extremes of the FFCE interaction needed to be defined to evaluate the computational and solid-state data generated by these studies. Two arenes were operationally defined as FFCE stacked if $\alpha < 45°$, $z < 4.6$ Å and if the vector originating at the ring center and normal to the plane of the ring at least met the edge of the atomic radius of the other ring. The normal vectors were found by averaging six cross products of pairs of vectors constructed from the centroid and the six atoms in the aromatic ring. Likewise, α was obtained from the dot products of the two normal vectors. The intramolecular stacking observed in **6(xtal)** failed these criteria. See Figures 2 and 3 for a depiction of the solid state intramolecular stacking in 5 and the only splayed conformation observed in this study found in **6-(xtal)**.

Table 1. N1–C2–C7–C8, the Biphenyl Dihedral Angle (deg) and C2–N1–C13–C14, the *N*-Benzyl Dihedral Angle (deg) and the Intramolecular Stacking Parameters α, *r*, *x*, and *z*[a]

	1	**2**	**3a**	**3b**	**3c**	**4**	**5**	**6**
N1–C2–C7–C8 (deg)	58.5	62.1	66.6	69.6	68.6	59.6	64.7	78.3
C2–N1–C13–C14 (deg)	58.8	70.8	65.4	66.6	72.4	64.8	48.8	71.0
α (deg)	28.1	33.7	23.2	25.1	37.7	39.2	22.5	16.0
r (Å)	4.07	4.39	4.16	4.10	4.42	4.33	3.61	4.34
x (Å)	2.01	2.14	2.23	2.02	2.84	1.96	1.22	3.07
z (Å)	3.54	3.83	3.51	3.57	3.39	3.86	3.40	3.06

[a] These are the dihedral angle between rings, the centroid to centroid distance, the horizontal displacement and the vertical displacement. There are three entries for **3** because there are three symmetry-unrelated molecules of **3** in the unit cell.

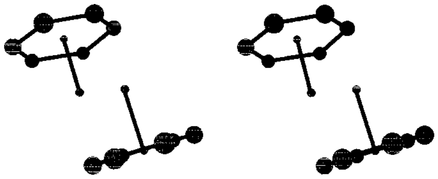

Figure 2. Stereoview of intramolecular stacking in **5** with unit vectors that are normal to and originate at the geometric center of each ring.

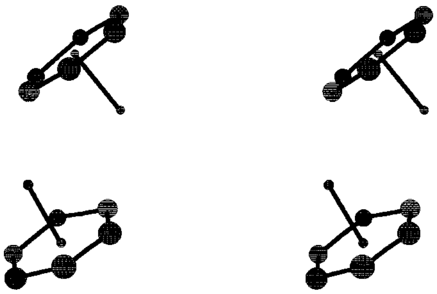

Figure 3. Stereoview of the intramolecular relationship between the benzyl and the phenyl rings in 6.

Calculations. Molecular modeling of **1** indicated that the biphenyl dihedral angle, N1–C2–C7–C8, needed to teeter between 57 and 72° to allow the phenyl substituent to swivel into interaction with the benzyl substituent. Calculations showed that molecules **1**–**8** should populate two conformations, a stacked conformation and a splayed conformation. With a continuum water dielectric implemented by MacromodelV5.0,[19] MM2* computationally probed the tendency of **1** to stack aromatic substituents as a function of two key dihedral angles. The counterion was not included in the calculations because solvent-

---

[18] Hoffmann, R. W. *Chem. Rev.* **1989**, *89*, 1841.

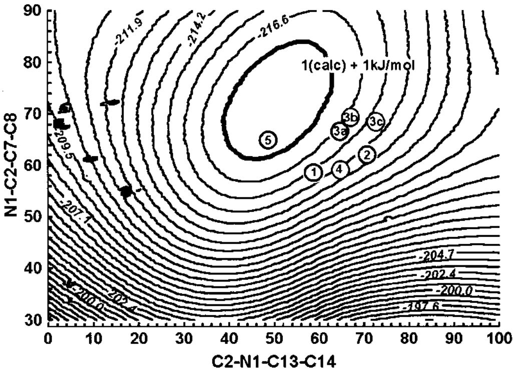

Figure 4. MM2* energy (kJ/mol) as a function of two dihedral angles (deg) for **1**. Conformations of **1(xtal)** − **5(xtal)** are labeled on the graph. There were three unique conformations for **3**.

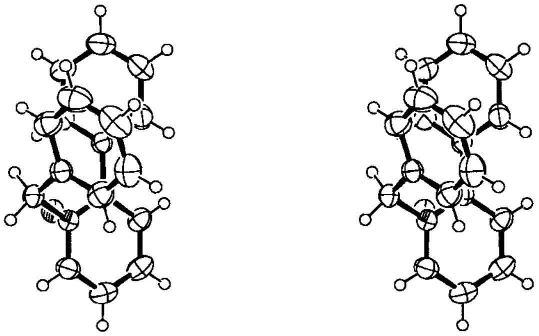

Figure 5. Stereoview of **1(xtal)**.

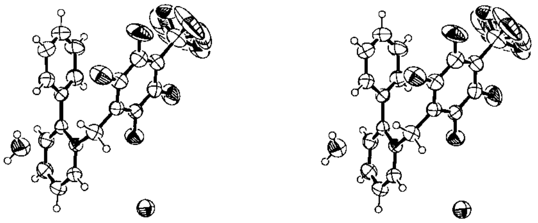

Figure 6. Stereoview of **5(xtal)**. This material crystallized with Br(−) and one H_2O in the unit cell.

separated ion pairs of **1** should have predominated in water. Increasing dihedral angles N1−C2−C7−C8 and C2−N1−C13−C14 (see Figure 1 for numeration) by 0.5° from 30° to 90° and from 0° to 180°, respectively, and minimizing the energy at each point generated a contour plot with 43,681 conformers. MM2* calculated structure **1(calc)** to reside in a shallow global minimum (N1−C2−C7−C8, 71°; C2−N1−C13−C14, 49°), and the splayed conformer of **1** occupied either a shallow local minimum or a saddle point. MM2* predicted the general conformation of the solid states, **1**−**5(xtal)** (labeled in Figure 4; ORTEP diagrams for **1**, **5**, and **6** are shown in Figures 5−7). The MM2* energy of the conformation of **1(xtal)** was found within 0.6 kcal/mol of **1(calc)**. However the analogous conformation of **5(xtal)** was found within 0.2 kcal/mol of **1(calc)**.

Using atomic coordinates from the crystal structures, **1**−**5** were minimized with PM3 semiempirical calculations. The structures converged on splayed conformations. For most of these PM3 calculations the difference in energy between stacked and splayed conformations was approximately 2 kcal/mol with a preference for the splayed conformation.

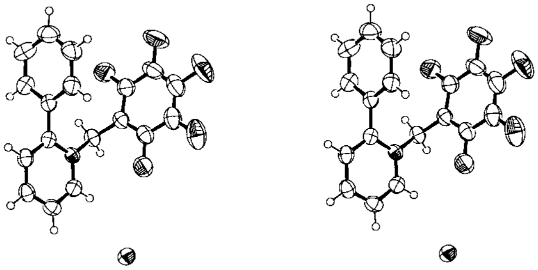

Figure 7. Stereoview of the **6(xtal)**.

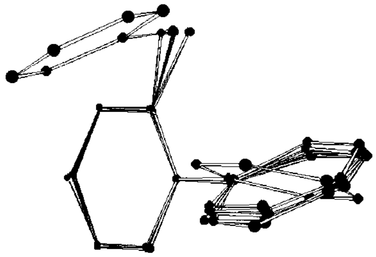

Figure 8. Rigid RMS superimposition of atoms C2, C4, and C6 of the solid-state conformations of **1**−**6**. The benzyl substituents of **2**−**6** were removed for clarity. The original coordinates or the enatiomers were used so all the benzyl substituents of **1** were on the same side of the pyridinium ring. The phenyl substituent in **6** does not overlap ortho and meta positions with the other rings.

Going to the 6-31G(d) level of theory decreased Δ*E* between **1(splayed)** and **1(stacked)** but did not change this preference of **5**. Perhaps additional levels of theory would better reflect Δ*E* between the stacked and splayed conformations. Probably ascension to the MP2 level of theory was needed to get accurate results for the long-range interactions necessary to describe the $\pi-\pi$ interactions. Currently, minimization at this level of theory is impractical.

Small biphenyl dihedral angles are often the result of packing interactions.[20] Unfortunately, the survey by Brock et. al. only dealt with biphenyl derivatives that were unsubstituted at the ortho positions. Such a survey of 2-substituted biphenyl or of pyridinium salts is unknown. The solid-state conformations of **1**−**6** were overlain in Figure 8 at C2, C4, and C6. Benzyl fragments on **2**−**6** were removed for clarity. To best compare the conformers, some structures were inverted to conserve the stereochemistry of the N1−C2−C7−C8 dihedral bond angle. The N1−C2−C7−C8 dihedral angles in **1**−**5** were nearly constant. The average biphenyl dihedral angle for **1**−**5** was 63 ± 4°. The solid-state conformation **6(xtal)** had N1−C2−C7−C8 = 78.3°. Packing interactions may have increased the difference in conformation between **5** and **6**. This notion is explored in the following paper in this issue.[27]

The conformations of **1(calc)** and **1**−**5(xtal)** were structurally related; **6(xtal)** was different and does not belong on the contour plot in Figure 4 because the relative pitches of the Bn and Ph rings are opposite to

---

[19] Mohamadi, F.; Richards, N. G. J.; Guida, W. C.; Liskamp, R.; Lipton, M.; Caufield, C.; Chang, G.; Hendrickson, T. S.; Still, W. C. *J. Comput. Chem.* **1990**, *11*, 440.

[20] Brock, C. P.; Minton, R. P. *J. Am. Chem. Soc.* **1989**, *111*, 4586−4593.

those found in **1**−**5(xtal)**. The C2−N1−C13−C14 dihedral angles in **1(xtal)** and **5(xtal)** are 58.5° and 48.8°, whereas this angle in **6(xtal)** increased to 260.8°. The conformation of **6(xtal)** did not satisfy the operational definition of any intramolecular stacking motif. The aromatic substituents in **6(xtal)** met at the edges, and these rings did not share significant face-to-face or edge-to-face surface area (see Figure 3).

Structures **1**−**5(xtal)** were obtained from moist *n*-BuOH; however, **6(xtal)** resulted from a deliberate attempt to change the solid-state morphology by crystallization from warm $MeNO_2$/toluene. Other $MeNO_2$/toluene crystallization attempts with **1**−**8** did not result in material suitable for diffraction. Likewise, suitable crystals of **6** were not had from the less esoteric procedures used for the other compounds. Suitable crystals of neither **7** nor **8** were obtained.

Structure **5(xtal)** optimized intramolecular π-stacking better than any of the other solid-state conformations (see Figure 2). Table 1 reports stacking parameters for the intramolecular relationships of the aryl substituents of these molecules in the solid state. Perfluoro substitution should have destabilized FFCE if the interaction of the opposite quadrupoles of the 2-phenyl and the perfluorobenzyl substituents are important in **6** and **5** versus **1** and **2**.[10,21] However, given the opportunity, **5** attained nearly canonical FFCE stacking in the solid state. Torsional constraints imposed by **1** should have favored the FFCE conformer or the splayed conformation. There are no close contacts in any of the crystal structures that would indicate that the conformations of **1**−**5** resulted from packing forces. However, the remote nature of the intramolecular stacking in **4** (note the high α in Table 1) was the result of intermolecular interaction. In this crystal, CF_3 from another molecule invaded the space that might otherwise have been occupied by the benzyl substituent stacking on the phenyl. The high α in **3c** in Table 1 also appears to the result from crystal packing. Crystal packing in **3** and **4** is explored in the following paper in this issue.

The solid state of **6** was unique in that it consisted of a noncovalent polymer in which Bn and Ph substituents were intermolecularly stacked. This interaction may have broken the intramolecular noncovalent interaction between the Bn and Ph rings.

NMR Studies. Derivatives of **1** showed a propensity to stack aromatic substituents in the solvated state. ^{1}H NMR chemical shifts for H8, H9, and H10 of **1**−**8** roughly correlated with the shielding tensor[23] of the benzyl ring in the conformation of **1(xtal)**. Substituent-dependent changes in chemical shift were referenced to analogous chemical shifts in *N*-ethyl-2-phenylpyridinium bromide (EtPhPy). For stacked structures, the shielding tensor[23] predicts that H8, H9, and H10 resonances should appear upfield from analogous protons of EtPhPy and $\Delta\delta_{ortho}$ should have been roughly three times bigger than $\Delta\delta_{meta}$, which in turn should have been three times bigger than $\Delta\delta_{para}$. Figure 9 shows that expectations in $\Delta\delta$ ^{1}H NMR matched observations. Similar upfield $\Delta\delta$ were observed in the comparison of the ^{1}H NMR spectra of *N*-benzylpyridinium bromide and **1**.[17] Figure **9** shows no dramatic change in conformation on going from **1** to perfluorinated **5** or **6**.

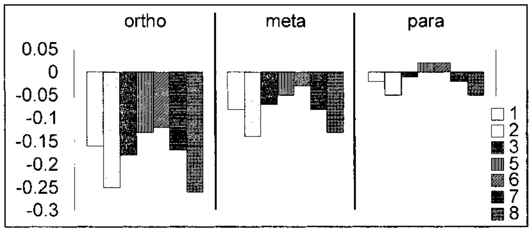

Figure 9. $\Delta\delta$ ^{1}H NMR of indicated derivatives of **1** in D_2O. Assignment by COSY and *J* values, referenced to *N*-ethyl-2-phenylpyridinium bromide (EtPhPy).

Further evidence for the family of stacked conformations in solution came from a NOESY study of **2** (3 °C, D_2O, 500 MHz). The cross-peak between H13 and H15 (H13−H15) should have been relatively invariant in both stacked and splayed conformations (see Figure 1 for atom numbers). H6−H13 was the most intense NOESY off-diagonal resonance separated by more than three bonds. If the splayed structure were the most populated, H8−H13 and H13−H15 should have dominated the spectrum. Concurrence of H6−H15 (weak), H8−H15 (weak), and H8−H16 (very weak) also indicated π-stacking. Peaks that did not appear on both dimensions were rejected.

Similar to Gellman's observations,[24] derivatives of **1** showed little change in conformation on going from aqueous conditions to DMSO. Trifluoroethanol, TFE, (15 mol %), a known water structure breaker,[25] also had little effect on the conformation of **1** by ^{1}H NMR. The ^{1}H NMR chemical shift apparently depended more on solvent access to the polar regions in the molecule and did not produce the solvent-dependent anisotropic field effects indicative of a population shift in conformation. ^{1}H NMR chemical shifts of EtPhPy were more sensitive to [TFE] than ^{1}H NMR chemical shifts of **1**−**8**.

Conclusion

Crystal structures, solution spectroscopic studies, and molecular modeling of the potential energy surface indicated that the title compounds served well as FFCE π-stacking models. Because the energy barriers between stacked and splayed conformations are low, perturbations in solvent conditions or perturbations from substitution should have biased conformational distributions if π-stacking depended greatly on solvation or on the substituents chosen. Solid-state perfluorobenzyl derivative **5** intramolecularly stacked Bn and Ph substituents in a canonical FFCE motif in the absence of close intermolecular packing interactions. This was strong evidence that derivatives of **1** template the FFCE motif as planned. Conformational insensitivity to substituents on the benzyl ring observed for **1**−**8** was reminiscent of a family of molecules explored by Wilcox.[11] In that study, the authors argued that dispersion forces are more important to solution phase π-stacking than the interaction of quadrupoles.

---

(21) Ngola, S. M.; Dougherty, D. A. *J. Org. Chem.* **1998**, *63*, 4566−67.

(22) Rappé, A. K.; Casewit, C. J. *Molecular Mechanics across Chemistry*; University Science Books: Sausalito, CA, 1997.

(23) Haigh, C. W.; Mallion, R. B. *Prog. NMR Spectrosc.* **1980**, *13*, 303−344.

(24) Newcomb, L. F.; Gellman, S. H. *J. Am. Chem. Soc.* **1994**, *116*, 4993−4994.

(25) Walgers, R.; Lee, T. C.; Cammers-Goodwin, A. *J. Am. Chem. Soc.* **1998**, *120*, 5073−79.

Future studies will focus on **1** as a substructural element in the design of water soluble foldameric materials for molecular recognition of polyanions.[26]

Experimental Section

NMR spectra were measured at 300 and 500 MHz. The NOESY spectrum of **2** was measured at 500 MHz at 3 °C with 200 ms mixing time. Data for X-ray crystallographic analysis of compounds **1**−**6** were collected at room temperature on a Nonius KappaCCD diffractometer.

Elemental analysis of hygroscopic materials is an inherently difficult task. C, H, N analysis was attempted on compounds **1**−**3**, **7**, and **8**. Three of the materials (**1**−**3**) submitted were from crystals from which structures were obtained. The %C and the %N correlated well with the expected values when the material was assumed to contain nonintegral stoichiometries of H_2O. Table 2 in the Supporting Information reports the raw numbers from C, H, N analysis, the expected values, and the corrected numbers from the inclusion of a nonintegral number of water molecules. The error between the raw values and the expected values and the corrected values also appears in Table 2 (Supporting Information). The corrected values for the elemental analysis were generated by minimizing the sum of the error between the raw and corrected values in %C and %N. Substance **3** has an H_2O in the expected value because one H_2O crystallized with each molecule of **3**.

The salts **1**−**8** were synthesized by benzylation of 2-phenylpyridine either as neat liquids or as concentrated solutions in DMF. The following is representative of the synthesis and purification of **1**−**8**. In general, a minimal amount of DMF was used in the benzylation of 2-phenylpyridine. The salts either precipitated from the reaction conditions or precipitated on addition of diethyl ether.

Commercially available 4-cyanobenzyl bromide (0.46 g, 2.35 mmol) and 2-phenylpyridine (0.80 g, 5.15 mmol) were dissolved in 10 mL of DMF. After the mixture was stirred at room temperature for 2 days, the precipitate (0.61 g, 1.74 mmol, 74%) was filtered and washed with ether. The material was recrystallized using wet butanol in an atmosphere of hexane at room temperature: mp 155−156 °C; ^{1}H NMR 300 MHz (D_2O, ppm), δ 5.90 (2H, s), 7.04 (2H, d, $J = 8.2$ Hz), 7.37 (2H, dd, $J = 7.2$ Hz, 1.4 Hz), 7.35 (2H, ddd, $J = 7.8$ Hz, 7.2 Hz, 1.4 Hz), 7.64 (1H, tt, $J = 7.8$ Hz, 1.4 Hz), 7.65 (2H, d, $J = 8.2$ Hz), 8.07 (1H, dd, $J = 8.0$ Hz, 1.4 Hz), 8.17 (1H, ddd, $J = 7.9$ Hz, 6.4 Hz, 1.4 Hz), 8.68 (1H, ddd, $J = 8.0$ Hz, 7.9 Hz, 1.3 Hz), 9.08 (1H, dd, $J = 6.4$ Hz, 1.3 Hz); ^{13}C NMR 75 MHz (D_2O, ppm) 64.7, 114.2, 121.7, 129.8, 130.5, 131.0, 131.4, 132.0, 134.0, 134.1, 135.8, 141.4, 149.1, 149.5, 158.9; IR KBr pellet 1456.4, 1570.2, 1623.9, 2229.1, 3025.8 cm^{-1}.

Acknowledgment. A.C.-G. thanks the NSF (CHE-9702287) for support of this work.

Supporting Information Available: Synthesis and characterization data for all new compounds, NOESY spectrum of **2**, and X-ray structures for **1**−**6(xtal)** are available. The solid-state structures are reported in greater detail in the following paper in this issue. This material is available free of charge via the Internet at http://pubs.acs.org.

JO9907641

---

(26) Gellman, S. H. *Acc. Chem. Res.* **1998**, *31*, 173.

(27) Martin, C.; Patrick, B. O.; Cammers-Goodwin, A. *J. Org. Chem.* **1999**, *64*, 7807.